Thin Film Microextraction Enables Rapid Isolation and Recovery of DNA for Downstream Amplification Assays

Derek R. Eitzmann, Marcelino Varona, and Jared L. Anderson*

Department of Chemistry, Iowa State University, Ames, Iowa 50011, United States

Abstract

Nucleic acid analysis has been at the forefront of the COVID-19 global health crisis where millions of diagnostic tests have been used to determine disease status as well as sequencing techniques that monitor the evolving genome of SARS-CoV-2. In this study, we report the development of a sample preparation method that decreases the time required for DNA isolation while significantly increasing the sensitivity of downstream analysis. Functionalized planar supports are modified with a polymeric ionic liquid sorbent coating to form thin film microextraction (TFME) devices. The extraction devices are shown to have high affinity for DNA while also exhibiting high reproducibility and reusability. Using quantitative polymerase chain reaction (qPCR) analysis, the TFME devices are shown to require low equilibration times, while achieving higher preconcentration factors than solid-phase microextraction (SPME) by extracting larger masses of DNA. Rapid desorption kinetics enable higher DNA recoveries using desorption solutions that are less inhibitory to qPCR and loop-mediated isothermal amplification (LAMP). To demonstrate the advantageous features of the TFME platform, a customized leuco crystal violet LAMP assay is used for visual detection of the ORF1ab DNA sequence from SARS-CoV-2 spiked into artificial oral fluid samples. When coupled to the TFME platform, 100% of LAMP reactions were positive for SARS-CoV-2 compared to 66.7% obtained by SPME for a clinically relevant concentration of 4.80×10^6 DNA copies/mL.

***Corresponding Author:**

Jared L. Anderson
Department of Chemistry
Iowa State University
1605 Gilman Hall
Ames, IA 50011
Email: andersoj@iastate.edu

Introduction

The analysis of nucleic acids (NAs) has been foundational for the development of modern genetics,[1] forensics,[2] and microbial diagnotisics.[3] The presence of NAs in biological samples is ubiquitous, but they are often difficult to isolate and may be in low abundance.[4] Sample preparation methods are typically required to isolate target NAs from the matrix in which they are found; however, collecting high purity NAs for subsequent analysis is a formidable challenge for many preconcentration techniques as their purity is crucial to downstream NA amplification-based analysis.[4-7] Impurities present within NA samples resulting from improper or insufficient sample preparation often decreases the reproducibility and accuracy of results from downstream assays.[8-10]

Commercial solid-phase extraction (SPE) kits are often used to purify NAs and require chaotropic salts to facilitate their adsorption onto the silica sorbent, followed by several washes prior to elution.[11] These kits lack reusability, require specialized equipment, and involve substantial user intervention.[10] Alternative sample preparation techniques are required to overcome these fundamental issues to achieve high throughput and cost-effective analysis. Solid-phase microextraction (SPME) is a promising technique that combines analyte isolation, clean-up, and preconcentration into a single step.[12, 13] SPE and SPME both utilize extraction phases to isolate analytes from the sample.[13] SPE differs by utilizing a large volume of extraction phase, typically in the form of a packed column, through which the sample is passed.[14] High analyte affinity to the extraction phase and a large sorbent volume-to-sample ratio can result in the exhaustive extraction of analyte(s) present in the sample.[14] SPME features an open format where the extraction phase is coated on a support and directly exposed to the sample in a significantly smaller volume-to-sample ratio.[13] This design limits the extraction process by controlling the transfer of analytes to the

extraction phase interface, providing higher efficiency and selectivity when sorbents possessing high affinity for desired analytes are used.[15] The amount of analyte in the extraction phase (n_e) eventually reaches equilibrium with the concentration of analyte in solution, as described by Eq. 1.[13]

$$n_e = K_{es} V_e C_s \qquad \text{Eq. 1}$$

The amount of analyte extracted is linearly related to the volume of the extraction phase (V_e), initial concentration of the analyte in the sample (C_s), and the distribution coefficient (K_{es}). In practice, equilibrium sampling by SPME can require long extraction times and may not significantly improve analyte sensitivity.[14] Extractions performed under non-equilibrium conditions can be used for quantification as the amount of analyte extracted is linearly related to the initial concentration in solution.[13, 14] For diffusion-limited extractions, the extraction rate is given by Eq. 2.[13]

$$\frac{N_e}{t} = \frac{D_s A_e}{\delta_s} C_s \qquad \text{Eq. 2}$$

The rate is determined by the surface area of the extraction phase (A_e), diffusion coefficient of the analyte (D_s), initial concentration of the analyte (C_s), and the diffusion layer thickness (δ_s). The diffusion layer thickness arises from analytes partitioning to the extraction phase, creating an analyte-deficient boundary layer where analytes in the bulk sample must diffuse before extraction.[13] Organic compounds such as polyaromatic hydrocarbons (PAHs) are often targeted by SPME devices, and their diffusion coefficients (~10^5 cm^2/s)[16] are approximately 10^{11} times larger than that of a 100 base-pair double-stranded DNA fragment (~2.0 x 10^{-7} cm^2/s).[17] Therefore, optimization of fundamental extraction parameters is imperative to selectively target DNA due to its inherently small diffusion coefficient.

Several extraction platforms have been optimized for use in a wide variety of applications. The cylindrical SPME geometry is highly versatile and has been adapted for water,[18, 19] food,[20, 21]

and in-vivo[22, 23] sampling. Magnetic stir bars have been coated with sorbents in stir bar sorptive extraction (SBSE) for the analysis of trace analytes in liquid samples.[24] The coated stir bars can be agitated to decrease the diffusion layer thickness and increase the sorption of analytes. Sorbent coatings have also been applied to planar geometries in thin film microextraction (TFME) to greatly enhance the sorbent surface area and sorption of analytes.[25] Bruheim and co-workers found that TFME enabled more sensitive detection of PAHs in headspace extractions compared to SPME.[25] The TFME platform was also benchmarked against SBSE by Qin and co-workers, where the former attained higher extraction rates and preconcentration when identical agitation speeds were used.[26] TFME has proven to be a versatile extraction platform for small molecules in environmental water,[25-27] oil,[28, 29] and biological samples.[30-33]

The design of sorbent coating materials is critical to achieve highly selective and efficient extraction of analytes. Effective sorbents must be robust, reproducible, and have high affinity for the targeted analyte(s). Recent studies have shown that polymeric ionic liquids (PILs) are compatible with biological samples while possessing high affinities for RNA and DNA.[34-37] Their affinity arises from electrostatic interactions as well as an anion-exchange mechanism in which halide counterions are exchanged with the negatively-charged phosphodiester backbone of NAs. NAs preconcentrated by the sorbent are then recovered in an aqueous salt solution where excess chloride anions desorb analyte from the sorbent. This class of sorbents have been successfully coupled to nucleic acid amplification assays such as quantitative polymerase chain reaction (qPCR) and isothermal amplification.[38-40] Loop-mediated isothermal amplification (LAMP) has been shown to amplify NAs faster and have lower equipment costs than qPCR.[41-43] Furthermore, LAMP can be coupled with colorimetric dyes for the qualitative detection of NAs without additional instrumentation requirements. [44-46]

Herein, we report a novel TFME platform featuring a PIL-based sorbent coating for the rapid extraction and analysis of DNA. The enhanced mass transfer provided by TFME facilitates faster and more sensitive DNA workflows. Using qPCR, extraction and desorption kinetics are studied for a series of three TFME devices containing various masses of the sorbent coating. Rapid desorption kinetics offered by TFME allow for improved recovery of DNA at lower salt concentrations compared to SPME, making it more appealing for use with downstream analysis methods such as liquid chromatography-mass spectrometry[47] and amplification assays. To demonstrate the advantages of the TFME platform, an optimized device was used to quickly isolate small amounts of DNA derived from the ORF1ab gene of SARS-CoV-2 in artificial oral fluid samples. After isolation, a colorimetric LAMP assay was developed for rapid visual detection.

Experimental

Preparation of TFME Devices and Scanning Electron Microscopy

All reagents and instrumentation used in this study are provided in the Supporting Information. Nitinol sheets (0.33 mm thickness) were acquired from Nexmetal (Sheridan, WY) and cut into 3.5 mm x 25 mm x 0.33 mm strips. The strips were functionalized with vinyltrimethoxysilane using a previously reported method.[48] The PIL was comprised of the [$C_9COOHVim^+$] [Br^-] IL monomer and [$C_{12}(Vim^+)_2$] 2[Br^-] IL crosslinker, shown in Figure S1, and have been employed in previous SPME studies due to its selectivity in extracting nucleic acids.[35, 37, 38] A PIL coating solution was prepared by adding 20.0 mg of IL monomer, 10.0 mg of IL crosslinker, and 10.0 μL of DAROCUR 1173 photoinitiator to 200.0 μL of methanol. A 5.0 μL volume of the coating solution was applied to an area of 3.5 mm x 20 mm on a functionalized nitinol strip, and placed in the photoreactor where solvent was evaporated using a fan for 5 minutes prior to initiating the lamps. Polymerization reactions were deemed complete after 5 minutes; this

process was repeated until the desired volume of coating solution was applied. For comparison, the same PIL was coated on a SPME fiber using a previously reported procedure.[35]

Prepared TFME and SPME devices were cut into segments using metal sheers and grounded to a graphite stage using copper tape. The samples were then sputter coated with 5 nm of iridium to avoid charging. The scanning electron microscope (SEM, Quanta-FEG 250, FEI, USA) was operated using an acceleration voltage of 10.00 kV. An Everhart-Thornley detector was used to detect secondary electrons for investigation of film morphology and thickness.

SPME and TFME Procedures

A schematic for the extraction procedure can be found in Figure S2. SPME and TFME sorbents were immersed in 1.0 mL of extraction solution composed of 2.00 mM Tris-HCl buffer (pH 8.00) and 1.0 μL BRAF template DNA in a 1.5 mL DNA LoBind tube. For extractions involving SPME, the cap was pierced with a needle allowing the sorbent to pass through and be immersed in the extraction solution. For extractions using TFME, the sorbents were placed directly inside the tube. All extractions were agitated with a digital vortex mixer (Fisher Scientific) at 2500 rpm for a specified period of time. The sorbent was then removed and placed into a volume of NaCl solution (0.350 - 2.00 M) for a time-course. Desorption volumes of 10.0 μL and 90.0 μL were used for SPME and TFME, respectively to fully immerse the sorbent material. Vessels used for the desorption step were 3D printed and customized for the TFME and SPME sorbents. All sorbents were placed in the desorption vessel for a time-course and then removed and exposed to saturated NaCl (6.14 M) for 1.5 hours before reuse. Prior to qPCR analysis, volumes of 5.0 μL from the SPME vessel and 10.0 μL from the TFME vessel were diluted to a final NaCl concentration of 200 mM. All DNA template preparation procedures as well as qPCR conditions are provided in the Supporting Information.

Assay Conditions for LAMP LCV Detection of SARS-CoV-2

LAMP of the SARS-CoV-2 gene fragment was performed by heating all reactions at 63.0 °C. Each reaction contained 2.0 μL of 200.0 mM Tris-HCl (pH 8.90), 100.0 mM ammonium sulfate, and 1.0 % Tween 20, 3.2 μL of 5.0 M betaine, 2.8 μL of 10.0 mM dNTPs, 1.6 μL of magnesium sulfate, 2.0 μL of 8,000 U/mL Bst WarmStart polymerase, 2.0 μL of a primer solution containing 16.0 μM FIP and BIP, 8.0 μM LB and LF, and 2.0 μM F3 and B3, 4.4 μL of 250.0 μM crystal violet and 15.0 mM sodium sulfite, and 1.0 μL of 20X Evagreen dye. To achieve a final volume of 20.0 μL, 1.0 μL of DNA and 350 mM KCl were added to the reactions. For no-template control (NTC) reactions, 1.0 μL of 350 mM KCl was added prior to heating.

Colorimetric reaction results were determined following image analysis of the reaction tubes using ImageJ Software (Bethesda, Maryland, USA). Intensities of the reactions were compared to the NTC using the Student's t-test to determine statistically significant differences between the data sets. Reactions were deemed negative if there was no statistical difference at the 99% confidence interval, or if the mean intensity was greater than the NTC. All remaining reactions were designated as positive.

3D Printing Conditions

The custom designed desorption vessels were modeled using Autodesk Inventor Professional 2020 software (San Rafael, CA, USA) and printed using an Ultimaker S3 FDM 3D Printer (Utrecht, Netherlands) with Ultimaker transparent polylactic acid (PLA, 2.85 mm), white acrylonitrile butadiene styrene (ABS, 2.85 mm), natural polypropylene (PP, 2.85 mm), and transparent nylon (2.85 mm) filaments. After a series of studies, PLA was chosen as the material of choice and printed using a layer height of 0.1 mm, 100 % infill density, and an extrusion temperature of 205 °C. The glass print bed temperature was maintained at 60 °C.

Results and Discussion

Preparation of TFME Devices

PIL-based sorbent coatings in SPME have been previously coupled with vortex agitation to drastically increase DNA sorption.[38] However, this approach is suited only for highly durable sorbent coatings as loss of the coating will decrease reproducibility and reusability. In this work, TFME devices were prepared with varying masses of PIL coating to determine its effect on the sorption of DNA. A 1x TFME device consisting of a single sorbent coating was prepared along with 4x and 16x devices containing four and sixteen coated layers, respectively. Images of the TFME and SPME devices, along with the mass of PIL sorbent coating, are shown in Figure 1.

Following extraction, the TFME or SPME device was withdrawn from solution, rinsed with water, and then placed into a desorption vessel containing an aqueous sodium chloride solution at a specific concentration. After the desorption time-course, the device was removed and the desorption solution diluted prior to qPCR analysis. In qPCR, reactions containing a higher DNA concentration result in amplification that is detected earlier in the thermocycling program, thereby yielding lower cycle of quantification (Cq) values. To relate the initial concentration of DNA to the Cq value, a seven-point calibration curve was constructed for the BRAF DNA template, as shown in Figure S3.

Creation of 3D Printed Desorption Vessels

When DNA is desorbed from the PIL-based extraction device, the solution must be diluted prior to qPCR to prevent NaCl-mediated inhibition of amplification.[49] Therefore, it is important to use small volumes of the desorption solution to minimize dilution of DNA and maximize preconcentration. However, the planar geometry of TFME is a poor match with traditional cylindrical vessels and requires excess volume of the desorption solution to completely submerge

the sorbent coating. To address this, a desorption vessel featuring rectangular internal dimensions of 4.0 x 1.5 x 20.0 mm was generated using 3D modeling software. An additional 3D model was constructed for SPME to mimic the optimized desorption vessels used in previous studies.[38] The TFME and SPME desorption vessels were both composed of identical printing materials to enable their direct comparison.

A benefit of producing desorption vessels by 3D printing is that a wide variety of commercially-available polymer materials can be used. Factors such as leeching of qPCR inhibitory components, physical defects of the vessel, and the polymer's chemical composition can influence the quantity and purity of DNA recovered during desorption.[50] In this study, the amount of DNA adsorbed to the vessel wall during desorption was examined for four common polymer materials. The free DNA concentration in a 1.00 M NaCl solution contained within the vessels was monitored throughout a time-course using qPCR to mimic desorption conditions for a PIL-based device. As shown in Figure S4, no significant differences in the amount of DNA recovered for short time intervals was observed among the tested polymers. Desorption vessels constructed of PLA (Figure S5) were used in all experiments in this study due to the ease of producing vessels with this filament material and its low adsorption of the DNA fragment.

Extraction Kinetics of DNA using TFME Devices

Using the custom 3D printed desorption vessels, extractions performed with the 1x, 4x, and 16x TFME devices were compared against SPME. Four replicate devices, designated as A,B,C, and D, were prepared for each device type to investigate their performance, reproducibility, and reusability. As shown in Figure S6, the obtained Cq values reveal significantly less device-to-device variation in extraction performance for TFME compared to SPME, with the small variation being attributed to the high reproducibility of the coating method. All devices in this study were

also shown to have high reusability with no significant decrease in extraction performance after greater than 50 extractions, as shown in Figure S7. The amount of isolated DNA appears to be equivalent across the 1x, 4x, and 16x devices, which possessed significantly different masses of PIL coating. The increased mass of sorbent coating should result in both an increase in extraction phase surface area and volume; therefore, variation in the extraction rate and total mass of DNA extracted would be expected across the TFME devices, according to Equations 1 and 2. By comparing devices with similar DNA extraction performance in Figure S8, the TFME platform isolated a higher concentration and an order of magnitude more total mass of DNA compared to SPME. Additionally, SPME contained more than double the mass of sorbent coating as the 1x-B TFME device, highlighting the superior DNA extraction efficiency achieved by the TFME platform.

To systematically examine the effect of sorbent mass on the extraction of DNA, sorption-time profiles were constructed using DNA concentrations of 102.0, 10.2, and 1.02 pg/mL. Figure 2A shows that devices with the largest sorbent surface area (i.e., 4x-B and 16x-A) exhibited higher extraction rates than the 1x-B TFME and SPME-A devices using an initial DNA concentration of 102.0 pg/mL. Similarly, the amount extracted at equilibrium is identical across the TFME devices indicating that the volume of the extraction phase is independent of the amount of DNA extracted under these concentrations (Figure 2A-2C). According to Equation 1, the volume of the extraction phase should be linearly related to the amount of analyte recovered under equilibrium conditions. However, this equation is not valid if the analyte concentration is significantly depleted during the extraction resulting in a decreased extraction rate until a plateau is reached, as described by Equation 2.

When the DNA concentration was reduced to 1.02 and 10.2 pg/mL, the sorption-time profiles were more similar for the devices. The reduced DNA concentration, compounded with the high extraction rates provided by vortex agitation, decreased the significance of the extraction phase's surface area. This can be observed in Figures 2B and 2C where similar profiles for TFME devices are achieved. It is important to note that the SPME-A device still exhibited slower initial extraction rates in these trials compared to all TFME devices (Figure 2B-2C).

Recovery of DNA from TFME Devices using Method of Successive Desorption

For sorbent-based methods requiring a desorption step, desorption kinetics are a key factor in the complete workflow. If large amounts of analyte are extracted by the sorbent but are not completely desorbed, analyte carryover will interfere with subsequent analyses. Desorption characteristics of the TFME and SPME devices were studied following an extraction of DNA under equilibrium conditions. The devices were placed in a series of five vessels and statically desorbed for increasing periods of time enabling stepwise monitoring of DNA recovery, as illustrated in Figure S9.

Among all devices, the 1x-B and 4x-B TFME devices yielded significantly higher initial desorption rates at the lowest initial concentration of DNA (Figure 3C). The rapid desorption of DNA suggests that shorter time is required to recover analyte from these devices. The 1x-B TFME device showed the steepest elution profiles for all concentrations examined (Figure 3A-3C). The 4x-B TFME device also displayed high initial recoveries (Figures 3A-3C), but produced the largest recoveries from 6 to 18 minutes using 1.02 pg/mL (Figure 3C). This result indicates that the 4x-B TFME device extracts more DNA than the 1x-B TFME device, but the DNA cannot be completely desorbed in a single desorption step. For this same concentration, the 16x-A TFME device produced lower recovery of DNA than the 4x-B TFME device from 1-18 minutes (Figure 3C).

When studying the largest DNA concentration (102.0 pg/mL), the desorption kinetics for the 4x-B and 16x-A TFME devices were identical, as observed in Figure 3A. These results indicate that a significant fraction of extracted DNA may be diffusing into the larger extraction phase of the 16x-A device, resulting in its poorer recovery during desorption when less total mass is extracted. Additionally, the SPME-A device exhibited sluggish kinetics and produced a similar elution profile as the 16x-A TFME device (Figure 3C) and eluted the largest amount of DNA from 32-64 minutes when 102 pg/mL BRAF DNA was used (Figure 3A).

To better understand these results, the surface morphologies and film thicknesses of the TFME sorbents were examined using scanning electron microscopy. Images showing cross-sectional and planar views of the devices are shown in Figures S10-S11. TFME devices possessing low amounts of PIL sorbent coating (1x and 4x) did not form homogenous films but rather exhibited the formation of isolated polymer patches (Figure S10) during the coating process. For the 16x TFME and SPME devices, no bare metal is observed revealing a coating morphology indicative of high surface area (Figure S11). These two sorbents were previously shown in Figure 3C to exhibit more sluggish desorption kinetics.

Effect of Salt Concentration on DNA Desorption Kinetics

The extraction mechanism of PIL sorbents requires the use of NaCl to facilitate desorption of DNA.[35] The use of high concentrations of NaCl enables high DNA recovery, short desorption times, and low carryover. However, NaCl can be inhibitory to qPCR by decreasing amplification efficiency.[4] Therefore, it is important to exploit the kinetic advantages of the TFME platform for the desorption of DNA by using the lowest NaCl concentration to minimize DNA dilution prior to qPCR.

Due to its rapid sorption kinetics, the 4x-B TFME device was studied using NaCl concentrations ranging from 350 - 2000 mM, as shown in Figure 4A-4C. When 350 mM was examined, the 4x-B TFME device initially eluted significantly more DNA, as shown in Figure 4A. Similar results are also observed when the concentration was increased to 500 mM (Figure 4B). The increased desorption of DNA at lower concentrations of NaCl can be attributed to the increased surface area-to-volume ratio of the 4x-B TFME device. The total mass recovered with 350 and 500 mM was less than 40% of the amount collected using 1000 mM (Figure 3C), indicating that lower concentrations of NaCl lead to slower rates of desorption. When the concentration of NaCl was increased to 2000 mM, SPME eluted higher concentrations of DNA at the 18 and 32 minute time points, as shown in Figure 4C. Increased salt concentration appears to provide an enhanced driving force capable of desorbing more analyte from the sorbent. However, this was not observed for TFME as it already possesses a higher surface area-to-volume ratio and rapid desorption kinetics.

Rapid Detection of ORF1ab gene from SARS-CoV-2 in Artificial Oral Fluid by LCV LAMP

To demonstrate the advantages of the TFME platform, a rapid sample workflow was developed for the detection of the ORF1ab gene from SARS-CoV-2 by colorimetric LAMP, using an artificial oral fluid matrix as the extraction solution. The total time for isolation and recovery was limited to less than two minutes, and the desorption salt concentration was lowered to 350 mM. Additionally, the amplification time for the LAMP assay was limited to 33 minutes. Given these parameters, extraction devices possessing rapid extraction and desorption kinetics are required to detect SARS-CoV-2.

TFME devices can be tailored in terms of support geometry, size, and sorbent coating mass. To demonstrate this versatility, a 4x TFME device was prepared by reducing the coating mass and

coating area by half, as represented in Figure S12. The extraction device (TFME-E) possesses similar extraction/desorption characteristics of the 4x TFME device while enabling a reduction in the desorption volume (Figure S13). This alteration was hypothesized to increase the amount of DNA recovered prior to downstream applications and enhance the sensitivity of the combined extraction and detection workflow for any DNA sample. To demonstrate the increased sensitivity, the TFME-E device allowed for enhanced detection of BRAF DNA by qPCR and enabled quantification of isolated DNA compared to the SPME-A device which could not achieve quantification (Figure S14).

The colorimetric LAMP assay was developed with primers from El-Tholoth et al.[51] and a lecuo crystal violet (LCV) colorimetric detection method developed by Miyamoto et. al.[46] LCV is an ideal colorimetric detection dye because of the colorless to blue-violet transition for negative to positive samples. Other colorimetric dyes produce various transitions which may be more difficult to interpret.[44, 45] For secondary detection, a fluorescent double-stranded DNA binding dye was employed to monitor the amplification of DNA in real-time and enables correlation with endpoint results. The concentration of potassium chloride (10.0 mM) in the LCV LAMP buffer was increased to 17.5 mM and allowed direct addition of a 350 mM desorption solution without diminishing the determination of endpoint LCV results. Control reactions of the customized LCV LAMP assay are shown in Figure S15A. The endpoint results were determined following image analysis using ImageJ (Figure S15B-S15C) which revealed a high intensity for the NTC reaction, and low intensities produced by positive reactions. To maintain continuity with the previous experiments, target ORF1ab DNA was utilized in all experiments rather than RNA template.

The TFME-E and SPME devices were coupled to the LCV LAMP assay to detect a DNA fragment of the SARS-CoV-2 ORF1ab gene in artificial oral fluid. Data from six extractions and

a total of eighteen reactions are provided in Table S2, which shows that 100% of LCV LAMP reactions coupled to the TFME-E device were positive compared to 66.7% with SPME-A device. The colorimetric reactions, corresponding amplification data, and the measured intensities by ImageJ for all reactions are provided in Figures S16-S21. The increased positivity for the TFME-E device is attributed to it isolating significantly more DNA than SPME leading to earlier amplification of LAMP reactions. Some reactions that were not deemed positive (Figures S18-S21) produced detectable fluorescence during amplification; however, the concentration of amplified DNA in these reactions was below the detection limit of LCV, which was previously reported to be 7.1 ng/µL.[46] Variability of replicate SPME-LAMP reactions in this experiment can be attributed to increased deviation in the amplification times when lower amounts of DNA are used.[52]

In clinical settings, oral fluid samples are treated with chemical agents, thermal lysis, or SPE kits to increase the amount of available nucleic acids for downstream reverse transcription leading to more sensitive detection of SARS-CoV-2.[53-55] To mimic conditions for a workflow utilizing TFME, a simple viral lysis protocol involving proteinase K was chosen to determine the limit of detection for the LCV LAMP assay. For this experiment, the dsDNA binding dye was removed from the LCV LAMP and the amplification time was increased to 45 minutes to enable detection limits of 4.80×10^2 copies/reaction (Figure S22). To maximize DNA recovery, the extraction time was increased to 4 minutes and the desorption utilized 1.00 M KCl for 10 minutes. The results of the extractions coupled to LCV LAMP reactions are shown in Figure 5. While both devices produced identical results for concentrations of 4.80×10^5 and 4.80×10^7 copies/mL, the TFME-E device demonstrated higher sensitivity by reproducibly achieving positive LCV LAMP

reactions for 4.80 x 10^6 copies/mL compared to only 66.7% achieved by the SPME-A device (Table S3).

Conclusions

Results from this study demonstrate that the TFME platform provides rapid isolation and desorption of DNA prior to downstream analysis when employing selective PIL-based sorbent coatings. TFME devices possessing less than half the amount of sorbent mass compared to SPME were shown to isolate a higher concentration and an order of magnitude more total mass of DNA. Faster extraction rates were achieved with TFME devices allowing for reduced analysis times and increased sensitivity. Additionally, rapid desorption kinetics enabled higher DNA recoveries using lower salt concentrations, which is less inhibitory to downstream amplification assays. The versatility of the TFME platform was demonstrated by optimizing the geometry of the device as well as employing 3D printed desorption vessels to facilitate visual detection of a DNA sequence originating from SARS-CoV-2 extracted from artificial oral fluid. Rapid extraction and desorption of DNA from thin sorbent films is highly attractive in the design of microfluidic devices featuring fast sample preparation and detection. We also envision that this approach could be highly useful in mass spectrometry applications where DNA can be eluted and directly analyzed or by exploiting the PIL-based sorbent as a matrix and performing matrix-assisted laser desorption/ionization (MALDI) analysis directly on the blade.

Acknowledgments

J.L.A. acknowledges funding from the Chemical Measurement and Imaging Program at the National Science Foundation (Grant No. CHE-1709372). J.L.A. and D.R.E. acknowledge the Alice Hudson Professorship for support.

Supporting Information

Reagents and instrumentation, DNA template preparation and qPCR conditions, list of primers and DNA sequences used, IL monomer and crosslinker, qPCR calibration curve, plots describing adsorption of DNA to 3D printed vessels, and images of desorption vessels. Extraction data for TFME and SPME, schematic of successive desorption experiment, SEM images of extraction devices are provided. A comparison of the TFME-E and 4x TFME devices, and endpoint LCV LAMP reactions with ImageJ analysis and real-time amplification results are provided.

References

1. Murphy, L. D.; Herzog, C. E.; Rudick, J. B.; Fojo, A. T.; Bates, S. E., Use of the Polymerase Chain Reaction in the Quantitation of mdr-1 Gene Expression. *J. Biochem.* **1990,** *929*, 10351-10356.
2. Gunn, P.; Walsh, S.; Roux, C., The nucleic acid revolution continues - Will forensic biology become forensic molecular biology? *Front. Genet.* **2014,** *5*, 44-44.
3. Josephson, K. L.; Gerba, C. P.; Pepper, I. L., Polymerase Chain Reaction Detection of Nonviable Bacterial Pathogens. *Appl. Environ. Microbiol.* **1993,** *59*, 3513-3515.
4. Schrader, C.; Schielke, A.; Ellerbroek, L.; Johne, R., PCR inhibitors-occurrence, properties and removal. *J. Appl. Microbiol.* **2012,** *113*, 1014-1026.
5. Christopoulos, T., Nucleic Acid Analysis. *Anal. Chem.* **1999,** *71*, 425R-438R.
6. Emaus, M.; Varona, M.; Eitzmann, D.; Hsieh, S.-A.; Zeger, V.; Anderson, J., Nucleic acid extraction: Fundamentals of sample preparation methodologies, current advancements, and future endeavors. *Trend Anal. Chem.* **2020,** *130*, 115985- 115985.
7. Demeke, T.; Jenkins, R., Influence of DNA extraction methods, PCR inhibitors and quantification methods on real-time PCR assay of biotechnology-derived traits. *Anal. Bioanal. Chem.* **2010**, 1977-1990.
8. Abbaszadegan, M.; Stewart, P.; LeChevallier, M., A Strategy for Detection of Viruses in Groundwater by PCR. *Appl. Environ. Microbiol.* **1999,** *65*, 444-449.
9. Mouliou, D. S.; Gourgoulianis, K. I., False-positive and false-negative COVID-19 cases: respiratory prevention and management strategies, vaccination, and further perspectives. *Expert Rev. Respir. Med.* **2021,** *15*, 993-1002.
10. Löffler, J.; Hebart, H.; Schumacher, U.; Reitze, H.; Einsele, H., Comparison of different methods for extraction of DNA of fungal pathogens from cultures and blood. *J. Clin. Microbiol.* **1997,** *35*, 3311-3312.
11. Boom, R.; Sol, C. J.; Salimans, M. M.; Jansen, C. L.; Wertheim-van Dillen, P. M.; van der Noordaa, J., Rapid and simple method for purification of nucleic acids. *J. Clin. Microbiol.* **1990,** *28*, 495-503.
12. Arthur, C.; Pawliszyn, J., Solid Phase Microextraction with Thermal Desorption Using Fused Silica Optical Fibers. *Anal. Chem.* **1990,** *62*, 2145-2148.

13. Reyes-Garcés, N.; Gionfriddo, E.; Gómez-Ríos, G. A.; Alam, M. N.; Boyacı, E.; Bojko, B.; Singh, V.; Grandy, J.; Pawliszyn, J., Advances in Solid Phase Microextraction and Perspective on Future Directions. *Anal. Chem.* **2018,** *90*, 302-360.
14. Prosen, H.; Zupančič-Kralj, L., Solid-phase microextraction. *Trend Anal. Chem.* **1999,** *18*, 272-282.
15. Qin, Z.; Mok, S.; Ouyang, G.; Dixon, D. G.; Pawliszyn, J., Partitioning and Accumulation Rates of Polycyclic Aromatic Hydrocarbons into Polydimethylsiloxane Thin Films and Black Worms from Aqueous Samples. *Anal. Chim. Acta* **2010,** *667*, 71-76.
16. Gustafson, K. E.; Dickhut, R. M., Molecular Diffusivity of Polycyclic Aromatic Hydrocarbons in Aqueous Solution. *J. Chem. Eng. Data* **1994,** *39*, 281-285.
17. Lukacs, G. L.; Haggie, P.; Seksek, O.; Lechardeur, D.; Freedman, N.; Verkman, A. S., Size-dependent DNA mobility in cytoplasm and nucleus. *J. Biol. Chem.* **2000,** *275*, 1625-1629.
18. Chen, J.; Pawliszyn, J., Solid Phase Microextraction Coupled to High-Performance Liquid Chromatography. *Anal. Chem.* **1995,** *67*, 2530-2533.
19. Piri-Moghadam, H.; Ahmadi, F.; Pawliszyn, J., A critical review of solid phase microextraction for analysis of water samples. *Trend Anal. Chem.* **2016,** *85*, 133-143.
20. Yang, X.; Peppard, T., Solid-Phase Microextraction for Flavor Analysis. *J. Agric. Food Chem* **1994,** *42*, 1925-1930.
21. Kataoka, H.; Lord, H. L.; Pawliszyn, J., Applications of solid-phase microextraction in food analysis. *J. Chromatogr. A.* **2000,** *800*, 35-62.
22. Bojko, B.; Gorynski, K.; Gomez-Rios, G. A.; Knaak, J. M.; Machuca, T.; Spetzler, V. N.; Cudjoe, E.; Hsin, M.; Cypel, M.; Selzner, M.; Liu, M.; Keshavjee, S.; Pawliszyn, J., Solid phase microextraction fills the gap in tissue sampling protocols. *Anal. Chim. Acta* **2013,** *803*, 75-81.
23. Lord, H. L.; Grant, R. P.; Walles, M.; Incledon, B.; Fahie, B.; Pawliszyn, J. B., Development and Evaluation of a Solid-Phase Microextraction Probe for in Vivo Pharmacokinetic Studies. *Anal. Chem.* **2003,** *75*, 5103-5115.
24. David, F.; Sandra, P., Stir bar sorptive extraction for trace analysis. *J. Chromatogr. A* **2007,** *1152*, 54-69.
25. Bruheim, I.; Liu, X.; Pawliszyn, J., Thin-Film Microextraction. *Anal. Chem.* **2003,** *75*, 1002-1010.
26. Qin, Z.; Bragg, L.; Ouyang, G.; Pawliszyn, J., Comparison of thin-film microextraction and stir bar sorptive extraction for the analysis of polycyclic aromatic hydrocarbons in aqueous samples with controlled agitation conditions. *J. Chromatogr. A* **2008,** *1196-1197*, 89-95.
27. Ayazi, Z.; Shekari Esfahlan, F.; Monsef Khoshhesab, Z., ZnO nanoparticles doped polyamide nanocomposite coated on cellulose paper as a novel sorbent for ultrasound-assisted thin film microextraction of organophosphorous pesticides in aqueous samples. *Anal. Methods* **2018,** *10*, 3043-3051.
28. Ye, C.; Wu, Y.; Wang, Z., Modification of cellulose paper with polydopamine as a thin film microextraction phase for detection of nitrophenols in oil samples. *RSC Adv.* **2016,** *6*, 9066-9071.
29. Ye, C.; Liu, C.; Wang, S.; Wang, Z., Investigation of 1-Dodecylimidazolium Modified Filter Papers as a Thin-Film Microextraction Phase for the Preconcentration of Bisphenol A from Plant Oil Samples. *Anal. Sci.* **2017,** *33*, 229-234.

30. Zargar, T.; Khayamian, T.; Jafari, M. T., Aptamer-modified carbon nanomaterial based sorption coupled to paper spray ion mobility spectrometry for highly sensitive and selective determination of methamphetamine. *Microchim. Acta* **2018,** *185*, 103-103.
31. Liu, F.; Xu, H., Development of a novel polystyrene/metal-organic framework-199 electrospun nanofiber adsorbent for thin film microextraction of aldehydes in human urine. *Talanta* **2017,** *162*, 261-267.
32. Zhang, H.; Hu, S.; Song, D.; Xu, H., Polydopamine-sheathed electrospun nanofiber as adsorbent for determination of aldehydes metabolites in human urine. *Anal. Chim. Acta* **2016,** *943*, 74-81.
33. Ríos-Gómez, J.; Lucena, R.; Cárdenas, S., Paper supported polystyrene membranes for thin film microextraction. *Microchem. J.* **2017,** *133*, 90-95.
34. Nacham, O.; Clark, K. D.; Anderson, J. L., Analysis of bacterial plasmid DNA by solid-phase microextraction. *Anal. Methods* **2015,** *7*, 7202-7207.
35. Nacham, O.; Clark, K. D.; Anderson, J. L., Extraction and Purification of DNA from Complex Biological Sample Matrices Using Solid-Phase Microextraction Coupled with Real-Time PCR. *Anal. Chem.* **2016,** *88*, 7813-7820.
36. Nacham, O.; Clark, K. D.; Varona, M.; Anderson, J. L., Selective and Efficient RNA Analysis by Solid-Phase Microextraction. *Anal. Chem.* **2017,** *89*, 10661-10666.
37. Varona, M.; Eitzmann, D. R.; Pagariya, D.; Anand, R. K.; Anderson, J. L., Solid-Phase Microextraction Enables Isolation of BRAF V600E Circulating Tumor DNA from Human Plasma for Detection with a Molecular Beacon Loop-Mediated Isothermal Amplification Assay. *Anal. Chem.* **2020,** *92*, 3346-3353.
38. Varona, M.; Ding, X.; Clark, K. D.; Anderson, J. L., Solid-Phase Microextraction of DNA from Mycobacteria in Artificial Sputum Samples to Enable Visual Detection Using Isothermal Amplification. *Anal. Chem.* **2018,** *90*, 6922-6928.
39. Varona, M.; Anderson, J. L., Visual Detection of Single-Nucleotide Polymorphisms Using Molecular Beacon Loop-Mediated Isothermal Amplification with Centrifuge-Free DNA Extraction. *Anal. Chem.* **2019,** *91*, 6991-6995.
40. Varona, M.; Eitzmann, D. R.; Anderson, J. L., Sequence-Specific Detection of ORF1a, BRAF, and ompW DNA Sequences with Loop Mediated Isothermal Amplification on Lateral Flow Immunoassay Strips Enabled by Molecular Beacons. *Anal. Chem.* **2021,** *93*, 4149-4153.
41. Notomi, T.; Okayama, H.; Masubuchi, H.; Yonekawa, T.; Watanabe, K.; Amino, N.; Hase, T., Loop-mediated isothermal amplification of DNA. *Nucleic Acids Res.* **2000,** *28*, e63-e63.
42. Parida, M.; Sannarangaiah, S.; Dash, P. K.; Rao, P. V.; Morita, K., Loop mediated isothermal amplification (LAMP): a new generation of innovative gene amplification technique; perspectives in clinical diagnosis of infectious diseases. *Rev. Med. Virol.* **2008,** *18*, 407-421.
43. Francois, P.; Tangomo, M.; Hibbs, J.; Bonetti, E.-J.; Boehme, C. C.; Notomi, T.; Perkins, M. D.; Schrenzel, J., Robustness of a loop-mediated isothermal amplification reaction for diagnostic applications. *FEMS Microbiol. Immunol.* **2011,** *62*, 41-48.
44. Goto, M.; Honda, E.; Ogura, A.; Nomoto, A.; Hanaki, K. I., Colorimetric detection of loop-mediated isothermal amplification reaction by using hydroxy naphthol blue. *BioTechniques* **2009,** *46*, 167-172.
45. Tanner, N. A.; Zhang, Y.; Evans, T. C., Visual detection of isothermal nucleic acid amplification using pH-sensitive dyes. *BioTechniques* **2015,** *58*, 59-68.

46. Miyamoto, S.; Sano, S.; Takahashi, K.; Jikihara, T., Method for colorimetric detection of double-stranded nucleic acid using leuco triphenylmethane dyes. *Anal. Biochem.* **2015,** *473*, 28-33.
47. Donato, P.; Cacciola, F.; Tranchida, P. Q.; Dugo, P.; Mondello, L., Mass spectrometry detection in comprehensive liquid chromatography: Basic concepts, instrumental aspects, applications and trends. *Mass Spectrom. Rev.* **2012,** *31*, 523-559.
48. Ho, T. D.; Toledo, B. R.; Hantao, L. W.; Anderson, J. L., Chemical immobilization of crosslinked polymeric ionic liquids on nitinol wires produces highly robust sorbent coatings for solid-phase microextraction. *Anal. Chim. Acta* **2014,** *843*, 18-26.
49. Kreader, C. A., Relief of amplification inhibition in PCR with bovine serum albumin or T4 gene 32 protein. *Appl. Environ. Microbiol.* **1996,** *62*, 1102-1106.
50. Pantazis, A. K.; Papadakis, G.; Parasyris, K.; Stavrinidis, A.; Gizeli, E., 3D-printed bioreactors for DNA amplification: application to companion diagnostics. *Sens. Actuators B Chem.* **2020,** *319*, 128161.
51. Song, J.; El-Tholoth, M.; Li, Y.; Graham-Wooten, J.; Liang, Y.; Li, J.; Li, W.; Weiss, S.R.; Collman, R.G.; Bau, H.H. Single- and Two-Stage, Closed Tube, Point-of-Care, Molecular Detection of SARS-CoV-2. *Anal. Chem.* **2021**, 93, 13063-13071.
52. Gandelman, O. A.; Church, V. L.; Moore, C. A.; Kiddle, G.; Carne, C. A.; Parmar, S.; Jalal, H.; Tisi, L. C.; Murray, J. A. H., Novel Bioluminescent Quantitative Detection of Nucleic Acid Amplification in Real-Time. *PLoS One* **2010,** *5*, e14155- e14155.
53. Moreno-Contreras, J.; Espinoza Marco, A.; Sandoval-Jaime, C.; Cantú-Cuevas Marco, A.; Barón-Olivares, H.; Ortiz-Orozco Oscar, D.; Muñoz-Rangel Asunción, V.; Hernández-de la Cruz, M.; Eroza-Osorio César, M.; Arias Carlos, F.; López, S.; Caliendo Angela, M., Saliva Sampling and Its Direct Lysis, an Excellent Option To Increase the Number of SARS-CoV-2 Diagnostic Tests in Settings with Supply Shortages. *J. Clin. Microbiol.* **2020,** *58*, e01659-20-e01659-20.
54. Rodríguez Flores, S. N.; Rodríguez-Martínez, L. M.; Reyes-Berrones, B. L.; Fernández-Santos, N. A.; Sierra-Moncada, E. J.; Rodríguez-Pérez, M. A., Comparison Between a Standard and SalivaDirect RNA Extraction Protocol for Molecular Diagnosis of SARS-CoV-2 Using Nasopharyngeal Swab and Saliva Clinical Samples. *Front. Bioeng. Biotechnol.* **2021,** *9*, 638902.
55. Lalli, M. A.; Langmade, J. S.; Chen, X.; Fronick, C. C.; Sawyer, C. S.; Burcea, L. C.; Wilkinson, M. N.; Fulton, R. S.; Heinz, M.; Buchser, W. J.; Head, R. D.; Mitra, R. D.; Milbrandt, J., Rapid and Extraction-Free Detection of SARS-CoV-2 from Saliva by Colorimetric Reverse-Transcription Loop-Mediated Isothermal Amplification. *Clin. Chem.* **2021,** *67*, 415-424.

Figure 1. Images of TFME and SPME devices with the corresponding mass of PIL sorbent coating. For TFME, a solution containing IL monomer, IL crosslinker, and photoinitiator was deposited, evaporated, and photo-polymerized on strips of functionalized nitinol metal. The sorbent coating for the 1x TFME device utilized one coating, whereas the 4x and 16x TFME devices required the process to be repeated for four or sixteen times, respectively. The top segment of TFME devices was left uncoated to enable their physical manipulation without disturbing the sorbent coating. For SPME, functionalized nitinol wire was affixed to a polyimide capillary for handling. The image of the SPME sorbent has been enlarged for easier viewing. The PIL coating can be observed as a tan color in all devices.

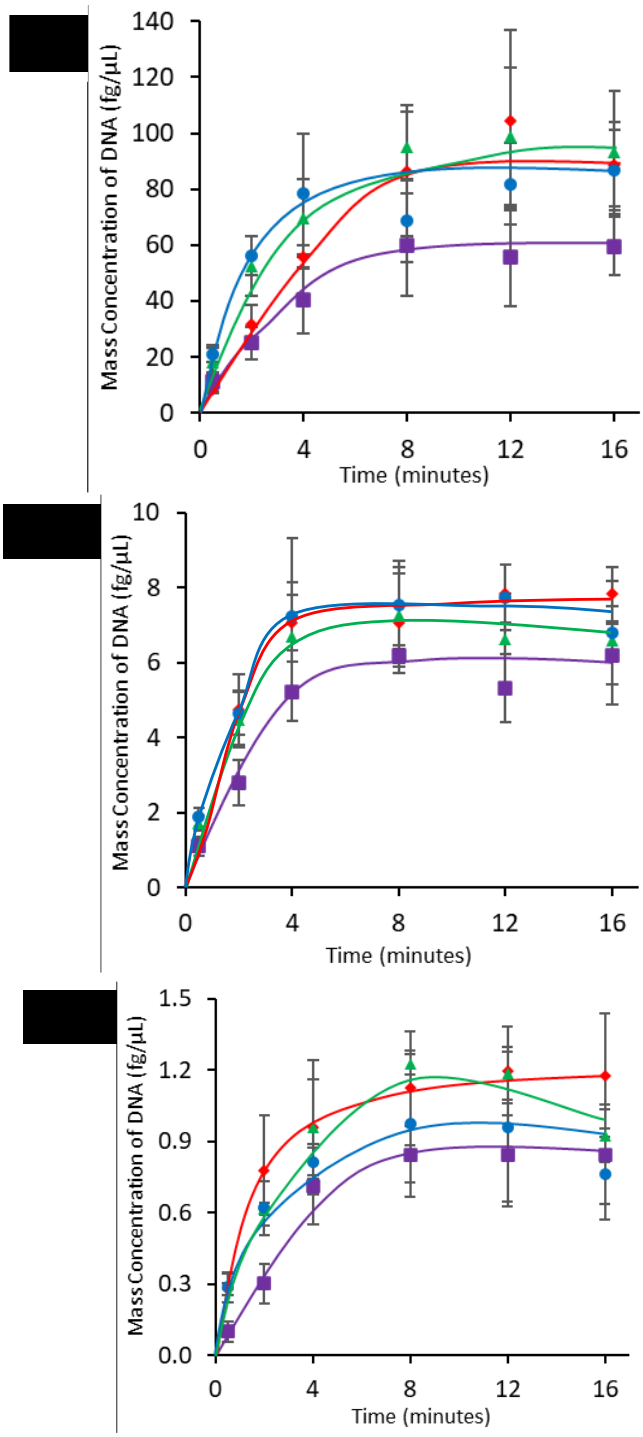

Figure 2: Extraction-time profiles for TFME and SPME devices containing PIL-based sorbent coatings. The initial DNA concentration in the extraction solution was (A) 102.0 pg/mL, (B) 10.2 pg/mL, and (C) 1.02 pg/mL. The extraction times were increased from thirty seconds to 16 minutes using vortex agitation at 2500 rpm. After extraction, the sorbents were desorbed in 1.00 M NaCl for 30 minutes. The Cq value was measured by qPCR and converted to mass concentration of DNA. The data is color-coded according to extraction device: TFME 1x-B (♦), TFME 4x-B (▲), TFME 16x-A (●), SPME-A (■).

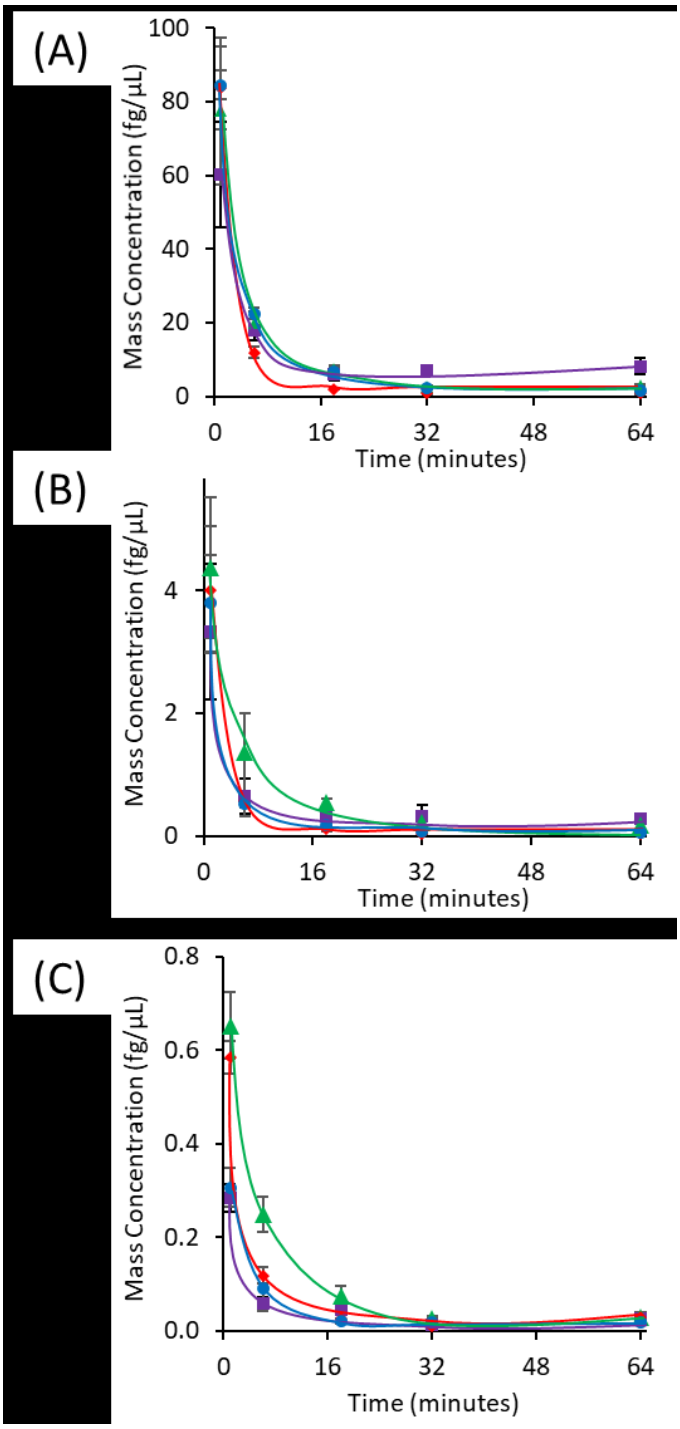

Figure 3. Successive desorption profiles for TFME and SPME devices. Extractions were performed with vortex agitation at 2500 rpm for 8 minutes using an extraction solution that contained (A) 102.0 pg/mL, (B) 10.2 pg/mL, or (C) 1.02 pg/mL DNA template. Desorption was carried out successively in 1.00 M NaCl in the first vessel for 1 minute, the second vessel for 5 minutes, third for 12 minutes, fourth for 14 minutes, and the fifth for 32 minutes (see Figure S8). Cq values were obtained from each desorption step and converted to the mass concentration of DNA. The data is color-coded according to extraction device: TFME 1x-B (♦), TFME 4x-B (▲), TFME 16x-A (●), SPME-A (■).

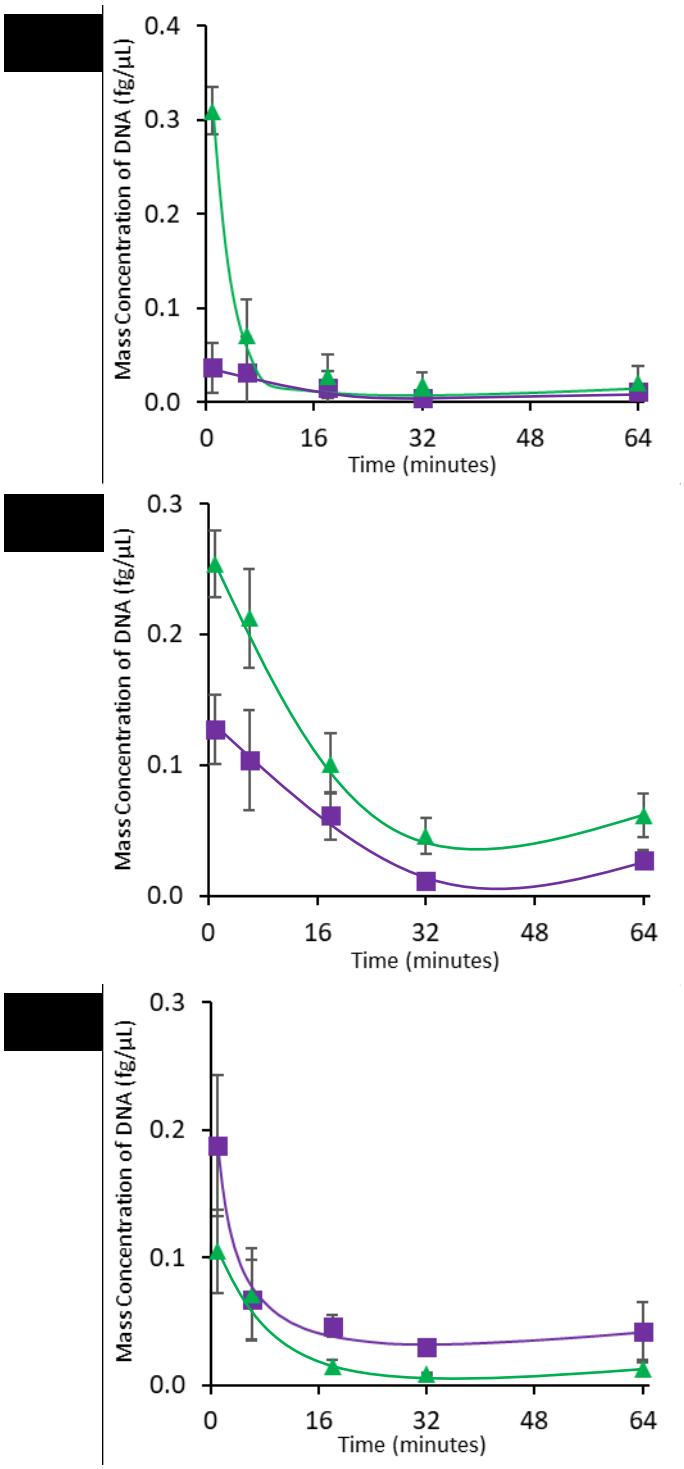

606

607

608

609 Figure 4. Desorption profiles of 4x-B TFME and SPME devices using increasing concentration
610 of NaCl in the desorption solution. The 1.00 mL extraction solution contained 1.02 pg/mL DNA
611 and devices were vortexed for 8 minutes at 2500 rpm. Desorption was carried out successively in
612 (A) 350 mM, (B) 500 mM, and (C) 2000 mM NaCl. Sorbents were washed and deposited into
613 five desorption vessels for increasing time from 1-32 minutes. Cq values were obtained from
614 each desorption by qPCR and converted to the mass concentration of DNA. The data is color-
615 coded according to extraction device: TFME 4x-B (▲), SPME-A (■).

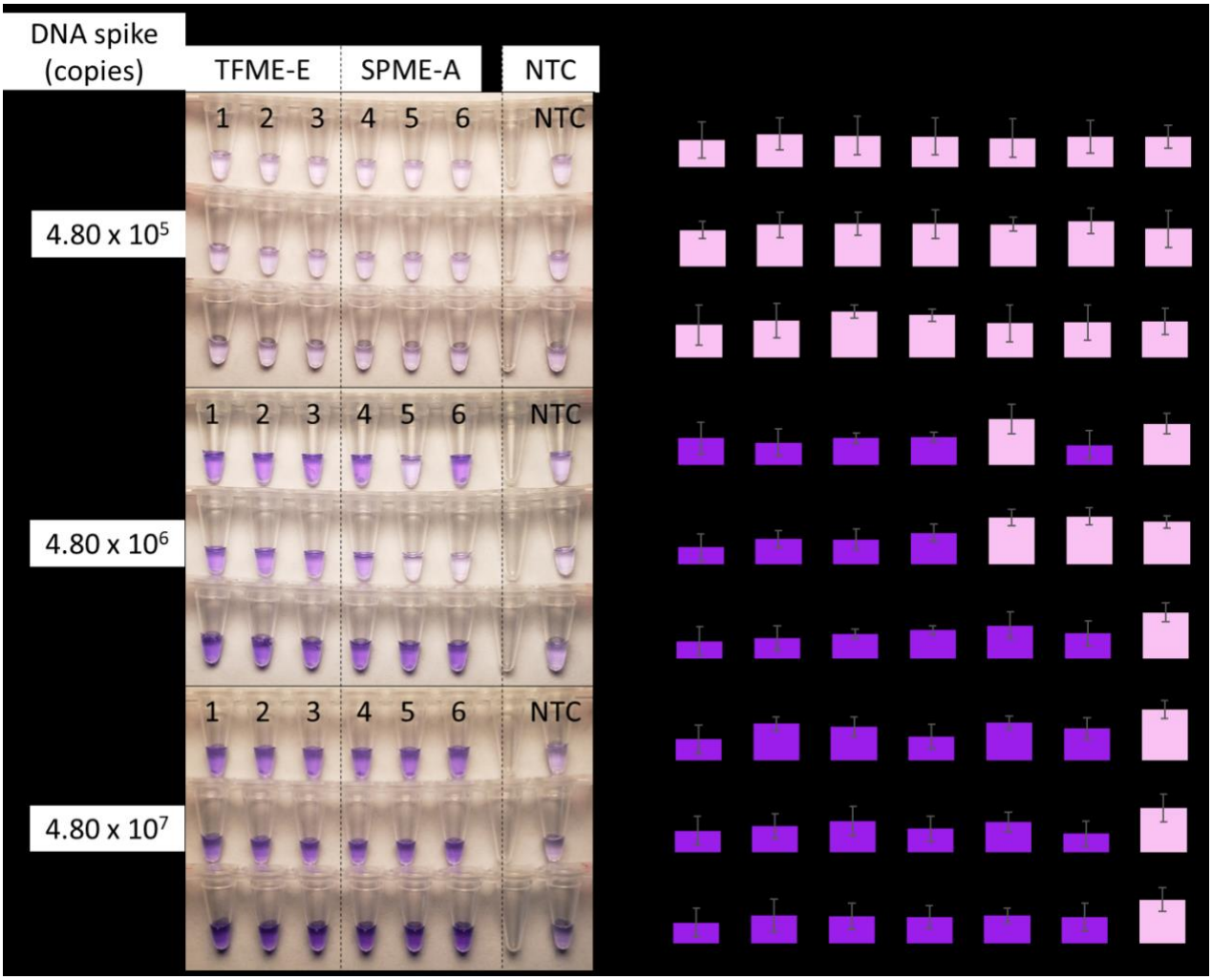

Figure 5. Comparison of TFME-E and SPME-A devices extracting decreasing amounts of ORF1ab gene fragment in artificial oral fluid following a viral lysis protocol. The extraction solution was composed of 910.0 µL of artificial oral fluid, 90.0 µL of proteinase K, and spiked DNA. The solution was heated to 65.0 °C for 15 minutes for enzyme activation, 95.0 °C for 5 minutes to deactivate the enzyme and, 25.0 °C for 5 minutes prior to the extraction. The extraction was carried out using a vortex mixer at 2500 rpm for 4 minutes and the desorption was carried out with 1.00 M KCl for 10 minutes. The desorption solution was diluted to 350 mM KCl prior to addition to a triplicate of LCV LAMP reactions which were carried out at 63.0 °C for 45 minutes. ImageJ analysis was conducted for determination and the intensities are displayed on the right side of the corresponding reactions; values shown in purple (■) have been determined to be positive, while values in pink (■) are negative.

634 **Table of Contents Image**

635